

PUMPING THE ECCENTRICITY OF EXOPLANETS BY TIDAL EFFECT

ALEXANDRE C.M. CORREIA

Department of Physics, I3N, University of Aveiro, Campus de Santiago, 3810-193 Aveiro, Portugal; and
 Astronomie et Systèmes Dynamiques, IMCCE-CNRS UMR8028, 77 Av. Denfert-Rochereau, 75014 Paris, France

GWENAËL BOUÉ

Centro de Astrofísica, Universidade do Porto, Rua das Estrelas, 4150-762 Porto, Portugal; and
 Astronomie et Systèmes Dynamiques, IMCCE-CNRS UMR8028, 77 Av. Denfert-Rochereau, 75014 Paris, France

AND

JACQUES LASKAR

Astronomie et Systèmes Dynamiques, IMCCE-CNRS UMR8028, 77 Av. Denfert-Rochereau, 75014 Paris, France
Draft version September 23, 2018

ABSTRACT

Planets close to their host stars are believed to undergo significant tidal interactions, leading to a progressive damping of the orbital eccentricity. Here we show that, when the orbit of the planet is excited by an outer companion, tidal effects combined with gravitational interactions may give rise to a secular increasing drift on the eccentricity. As long as this secular drift counterbalances the damping effect, the eccentricity can increase to high values. This mechanism may explain why some of the moderate close-in exoplanets are observed with substantial eccentricity values.

Subject headings: celestial mechanics — planetary systems — planets and satellites: general

1. INTRODUCTION

Close-in exoplanets, as for Mercury, Venus and the majority of the natural satellites in the Solar System, are supposed to undergo significant tidal interactions, resulting that their spins and orbits are slowly modified. The ultimate stage for tidal evolution is the synchronization of the spin and the circularization of the orbit (e.g. Correia 2009). The spin evolves in a shorter time-scale than the orbit, so long-term studies on the tidal evolution of exoplanets usually assume that their rotation is synchronously locked, and therefore limit the evolution to the orbits. However, these two kinds of evolution cannot be dissociated because the total angular momentum must be conserved. Synchronous rotation can only occur when the eccentricity is very close to zero. Otherwise, the rotation rate tends to be locked with the orbital speed at the periapsis, because tidal effects are stronger when the two bodies are closer to each other. In addition, in presence of a companion body, the eccentricity undergoes oscillations (e.g. Mardling 2007), and the rotation rate of the planet shows variations that follow the eccentricity (Correia & Laskar 2004). As a consequence, some unexpected behaviors can be observed, such as a secular increase of the eccentricity. In this Letter we provide a simple averaged model for the orbital and spin evolution of an exoplanet with a companion (Sect. 2), and apply it to the HD 117618 planetary system (Sect. 3). We then give an explanation for the eccentricity pumping (Sect. 4), and derive some conclusions (Sect. 5).

2. THE MODEL

We consider here a system consisting of a central star of mass m_0 , an inner planet of mass m_1 , and an outer companion of mass m_2 . We use Jacobi canonical coordi-

nates, with \mathbf{r}_1 being the position of m_1 relative to m_0 , and \mathbf{r}_2 the position of m_2 relative to the center of mass of m_1 and m_0 . We further assume that $|\mathbf{r}_1| \ll |\mathbf{r}_2|$, that the system is coplanar, and that the obliquity of the planet is zero. The inner planet is considered an oblate ellipsoid with gravity field coefficients given by J_2 , rotating about the axis of maximal inertia, with rotation rate ω , such that (e.g. Lambeck 1988)

$$J_2 = k_2 \frac{\omega^2 R^3}{3Gm_1}. \quad (1)$$

G is the gravitational constant, R is the radius of the planet, and k_2 is the second Love number for potential.

Since we are interested in the secular behavior of the system, we average the motion equations over the mean anomalies of both orbits. The averaged potential, quadrupole-level for the spin (e.g. Correia & Laskar 2010a), octopole-level for the orbits (e.g. Lee & Peale 2003; Laskar & Boué 2010), and with general relativity corrections (e.g. Touma et al. 2009) is given by:

$$U = -C_0(1 - e_1^2)^{-1/2} - C_1(1 - e_1^2)^{-3/2} - C_2 \frac{(1 + \frac{3}{2}e_1^2)}{(1 - e_2^2)^{3/2}} + C_3 \frac{e_1 e_2 (1 + \frac{3}{4}e_1^2)}{(1 - e_2^2)^{5/2}} \cos \varpi, \quad (2)$$

where

$$C_0 = \frac{3\beta_1 G^2 (m_0 + m_1)^2}{a_1^2 c^2}, \quad C_1 = \frac{G m_0 m_1 J_2 R^2}{2a_1^3}, \quad (3)$$

$$C_2 = \frac{G\beta_1 m_2 a_1^2}{4a_2^3}, \quad C_3 = \frac{15G\beta_1 m_2 a_1^3 (m_0 - m_1)}{16a_2^4 (m_0 + m_1)}. \quad (4)$$

a_i is the semi-major axis (that can also be expressed using the mean motion n_i), e_i is the eccentricity, and

$\varpi = \varpi_1 - \varpi_2$ is the difference between the longitudes of the periastron, ϖ_i . We also have $\beta_1 = m_0 m_1 / (m_0 + m_1)$, and $\beta_2 = (m_0 + m_1) m_2 / (m_0 + m_1 + m_2)$.

The contributions to the orbits are easily obtained using the Lagrange planetary equations (e.g. Murray & Dermott 1999):

$$\dot{e}_i = \frac{\sqrt{1-e_i^2}}{\beta_i n_i a_i^2 e_i} \frac{\partial U}{\partial \varpi_i}, \quad \dot{\varpi}_i = -\frac{\sqrt{1-e_i^2}}{\beta_i n_i a_i^2 e_i} \frac{\partial U}{\partial e_i}. \quad (5)$$

Thus,

$$\dot{e}_1 = -\nu_{31} \frac{e_2(1+3/4e_1^2)\sqrt{1-e_1^2}}{(1-e_2^2)^{5/2}} \sin \varpi, \quad (6)$$

$$\dot{e}_2 = \nu_{32} \frac{e_1(1+3/4e_1^2)}{(1-e_2^2)^2} \sin \varpi, \quad (7)$$

and

$$\begin{aligned} \dot{\varpi} = & \frac{\nu_0}{(1-e_1^2)} + \frac{\nu_1 x^2}{(1-e_1^2)^2} \\ & + \nu_{21} \frac{\sqrt{1-e_1^2}}{(1-e_2^2)^{3/2}} - \nu_{22} \frac{(1+\frac{3}{2}e_1^2)}{(1-e_2^2)^2} \\ & - \nu_{31} \frac{e_2 \sqrt{1-e_1^2} (1+\frac{9}{4}e_1^2)}{e_1 (1-e_2^2)^{5/2}} \cos \varpi \\ & + \nu_{32} \frac{e_1 (1+\frac{3}{4}e_1^2) (1+4e_2^2)}{e_2 (1-e_2^2)^3} \cos \varpi, \end{aligned} \quad (8)$$

where $x = \omega/n_1$, and the constant frequencies

$$\nu_0 = 3n_1 \left(\frac{n_1 a_1}{c} \right)^2, \quad (9)$$

$$\nu_1 = n_1 \frac{k_2}{2} \frac{m_0 + m_1}{m_1} \left(\frac{R}{a_1} \right)^5, \quad (10)$$

$$\nu_{21} = n_1 \frac{3}{4} \frac{m_2}{m_0 + m_1} \left(\frac{a_1}{a_2} \right)^3, \quad (11)$$

$$\nu_{22} = n_2 \frac{3}{4} \frac{m_0 m_1}{(m_0 + m_1)^2} \left(\frac{a_1}{a_2} \right)^2, \quad (12)$$

$$\nu_{31} = n_1 \frac{15}{16} \frac{m_2}{m_0 + m_1} \frac{m_0 - m_1}{m_0 + m_1} \left(\frac{a_1}{a_2} \right)^4, \quad (13)$$

$$\nu_{32} = n_2 \frac{15}{16} \frac{m_0 m_1}{(m_0 + m_1)^2} \frac{m_0 - m_1}{m_0 + m_1} \left(\frac{a_1}{a_2} \right)^3. \quad (14)$$

Notice that the variations in e_1 and e_2 (Eqs. 6, 7) are related by the conservation of the total angular momentum (after dividing by $m_1 n_2 a_2^2$):

$$\xi \frac{\omega}{n_2} \left(\frac{R}{a_2} \right)^2 + \frac{\beta_1}{m_1} \frac{n_1}{n_2} \left(\frac{a_1}{a_2} \right)^2 \sqrt{1-e_1^2} + \frac{\beta_2}{m_1} \sqrt{1-e_2^2} = Cte, \quad (15)$$

where ξ is a structure coefficient. The conservative system (Eq. 2) can thus be reduced to one degree of freedom.

In our model, we additionally consider tidal dissipation raised by the central star on the inner planet. The dissipation of the mechanical energy of tides in the planet's

interior is responsible for a time delay Δt between the initial perturbation and the maximal deformation. As the rheology of planets is badly known, the exact dependence of Δt on the tidal frequency is unknown. Several models exist (for a review see Correia et al. 2003; Efroimsky & Williams 2009), but for simplicity we adopt here a model with constant Δt , which can be made linear (Singer 1968; Mignard 1979). The contributions to the equations of motion are given by (e.g. Correia 2009):

$$\frac{\dot{\omega}}{n_1} = -K (f_1(e_1)x - f_2(e_1)), \quad (16)$$

$$\frac{\dot{a}_1}{a_1} = 2K' (f_2(e_1)x - f_3(e_1)), \quad (17)$$

$$\dot{e}_1 = 9K' \left(\frac{11}{18} f_4(e_1)x - f_5(e_1) \right) e_1, \quad (18)$$

where

$$K = n_1 \frac{3k_2}{\xi Q} \frac{m_0 \beta_1}{m_1^2} \left(\frac{R}{a_1} \right)^3, \quad K' = \frac{K}{1/\xi} \frac{m_1}{\beta_1} \left(\frac{R}{a_1} \right)^2, \quad (19)$$

$Q^{-1} = n_1 \Delta t$, and $f_1(e) = (1+3e^2+3e^4/8)/(1-e^2)^{9/2}$, $f_2(e) = (1+15e^2/2+45e^4/8+5e^6/16)/(1-e^2)^6$, $f_3(e) = (1+31e^2/2+255e^4/8+185e^6/16+25e^8/64)/(1-e^2)^{15/2}$, $f_4(e) = (1+3e^2/2+e^4/8)/(1-e^2)^5$, $f_5(e) = (1+15e^2/4+15e^4/8+5e^6/64)/(1-e^2)^{13/2}$.

We neglect the effect of tides over the longitude of the periastron, as well as the flattening of the central star. Their effect is only to add a small supplementary frequency to ϖ_1 , similar to the contributions from the general relativity (for a complete model see Correia et al. 2011).

Under the effect of tides alone, the equilibrium rotation rate, obtained when $\dot{\omega} = 0$, is attained for (Eq. 16):

$$\frac{\omega}{n_1} = f(e_1) = \frac{f_2(e_1)}{f_1(e_1)} = 1 + 6e_1^2 + \mathcal{O}(e_1^4). \quad (20)$$

Usually $K' \ll K$, so tidal effects modify the rotation rate much faster than the orbit. It is thus tempting to replace the equilibrium rotation in expressions (17) and (18). With this simplification, one obtains always negative contributions for \dot{a}_1 and \dot{e}_1 (Correia 2009),

$$\frac{\dot{a}_1}{a_1} = -7K' f_6(e_1) e_1^2, \quad (21)$$

$$\dot{e}_1 = -\frac{7}{2} K' f_6(e_1) (1-e_1^2) e_1, \quad (22)$$

with $f_6(e) = (1+45e^2/14+8e^4+685e^6/224+255e^8/448+25e^{10}/1792)(1-e^2)^{-15/2}/(1+3e^2+3e^4/8)$. Thus, the semi-major axis and the eccentricity can only decrease until the orbit of the planet becomes circular (Fig. 1a). However, planet-planet interactions can produce eccentricity oscillations with a period shorter, or comparable to the damping timescale of the spin. In that case, the expression (20) is not satisfied and multi-planetary systems may show non-intuitive eccentricity evolutions, such as eccentricity pumping of the inner orbit (e_1 increases while e_2 decreases).

TABLE 1
SINGLE PLANETARY SYSTEMS WITH $0.1 < a_1 < 0.3$ AND $e_1 > 0.3$.

Star (name)	a_1 (AU)	e_1	m_1 (M_J)	m_0 (M_\odot)	Age (Gyr)	τ (Gyr)
HD 108147	0.102	0.53	0.26	1.19	2.0	0.01
CoRoT-10	0.105	0.53	2.75	0.89	3.0	0.24
HD 33283	0.145	0.48	0.33	1.24	3.2	0.34
HD 17156	0.163	0.68	3.19	1.28	3.4	0.44
HIP 57050	0.164	0.31	0.30	0.34	—	39.4
HD 117618	0.176	0.42	0.18	1.05	3.9	2.06
HD 45652	0.228	0.38	0.47	0.83	—	93.3
HD 90156	0.250	0.31	0.06	0.84	4.4	35.8
HD 37605	0.260	0.74	2.84	0.80	10.7	10.6
HD 3651	0.284	0.63	0.20	0.79	5.1	15.5

NOTE. — Data is taken from <http://exoplanet.eu/>

$$\tau = \frac{2m_1 a_1^8 (1-e_1^2)^8}{\Delta t 21 k_2 G m_0^2 R^5}, \text{ with } \Delta t = 10^2 \text{ s (Correia \& Laskar 2010b).}$$

3. APPLICATION TO EXOPLANETS

As an illustration of the eccentricity pumping, we apply our model to the HD 117618 system. This Sun-like star ($m_0 \approx M_\odot$) has been reported to host a single Saturn-like planet on a eccentric orbit (Butler et al. 2006). The residuals of the best fitted solution to the observational data are 5.5 m/s, so we assume that any additional companion with a doppler shift semi-amplitude smaller than this value is presently undetected, that is, any planet with $m_2 < 0.2 M_J$ and $a_2 > 1.4$ AU.

In our simulations we adopt for the observed planet the same geophysical parameters as for Saturn, $R = R_{Sat}$, $k_2 = 1/2$, $\xi = 1/5$, and a dissipation time lag $\Delta t = 200$ s (which is equivalent to $Q \approx 3 \times 10^4$). Since the semi-major axis of the planet undergoes tidal dissipation, its value was certainly larger when the system formed. We then adopt $a_1 = 0.25$ AU as initial value for all simulations. The initial eccentricity is chosen such that $e_1 \approx 0.4$ when $a_1 = 0.175$, the present observed values (Tab. 1). We further assume initial $\varpi = 180^\circ$, and $2\pi/\omega = 50$ day, that quickly evolves near the equilibrium rotation (Eq. 20).

In absence of a companion, the eccentricity and the semi-major axis are damped following an exponential decay (Correia & Laskar 2010b), and the present configuration is attained after 1 Gyr (Fig. 1a). At present the observed eccentricity would be around 0.1, and we still needed to explain the high initial value near 0.7.

We now add a companion to the system with $m_2 = 0.2 M_J$, $a_2 = 1.8$ AU, and $e_2 = 0.4$, and set $e_1 = 0.3$. At first, we only consider dissipation in the spin (Eq. 16) and neglect its effect on the orbit (Eqs. 17, 18), in order to highlight the eccentricity pumping (Fig. 1b). We then clearly observe this effect, the eccentricity of the inner planet rising up to 0.7. We also observe that the eccentricity of the outer planet is simultaneously damped, because of the conservation of the total angular momentum (Eq. 15).

Orbital and spin evolution cannot be dissociated, so we then integrate the full system (Fig. 1c). We observe that the initial behavior of the system is identical to the situation without dissipation on the orbit (Fig. 1b). However, as the eccentricity increases, the inner planet comes closer to the star at periastron, and tidal effects on the orbit become stronger. As a consequence, the semi-major axis decreases and the damping effect on the eccentricity

(Eq. 18) overrides the pumping drift. The system ultimately evolves into a circular orbit. The present configuration is attained around 4 Gyr of evolution, which is compatible with the present estimated age of the star. The pumping effect is then responsible for a delay in the final evolution of planetary systems and may explain the high values observed for some of them (Tab. 1).

Finally, we repeat the integration of the full system, but with a smaller-mass companion $m_2 = 0.15 M_J$ at $a_2 = 1.4$ AU. The companion eccentricity is still $e_2 = 0.4$, but the inner planet now begins with $e_1 = 0.15$ (Fig. 1d). The initial evolution is still similar to the previous simulation (Fig. 1c), except that the eccentricity oscillations of both planets are higher, because the orbits are closer. Since the companion mass is smaller, its eccentricity also decreases more than before, and reaches zero around 3 Gyr. At this stage, the angle ϖ stops circulating, and begins librating around 180° . The two orbits are then tightly coupled and evolve together, showing an identical behavior to close-in planets with a few days of orbital period (e.g. Mardling 2007; Laskar et al. 2011). As a consequence, the evolution time-scale is much longer, allowing the inner planet to maintain high eccentricity for longer periods of time (Fig. 1d). The present eccentricity is only observed after 6 Gyr.

4. ECCENTRICITY PUMPING

In order to understand the unexpected behavior of the eccentricity during the initial stages of the evolution, we can perform some simplifications in the equations of motion without loss of generality (Sect. 2). We can neglect tidal effects on orbital quantities (Eqs. 17, 18), which is justified since $K' \ll K$ (Eq. 19). The only contribution of tides is then on the rotation rate (Eq. 16). The semi-major axis and the mean motion are thus constant, and the eccentricity only varies due to the gravitational perturbations (Eq. 6). In addition, we linearize the set of equations of motion in the vicinity of the averaged values of x , e_1 , and e_2 . Let $x = x_0 + \delta x$, where x_0 is the solution of (20), $e_1 = e_{10} + \delta e_1$, and $e_2 = e_{20} + \delta e_2$. In the following, δe_2 is expressed as a function of δx and δe_1 using the conservation of the angular momentum (Eq. 15). Then, the set of equations of motion (6, 8, 16) reduces to:

$$\delta \dot{e}_1 = -A \sin \varpi, \quad (23)$$

$$\dot{\varpi} = g + g_x \delta x + g_e \delta e_1, \quad (24)$$

$$\delta \dot{x} = -\nu_x \delta x + \nu_e \delta e_1, \quad (25)$$

with

$$A = \nu_{31} \frac{e_{20}(1 + 3/4 e_{10}^2) \sqrt{1 - e_{10}^2}}{(1 - e_{20}^2)^{5/2}}, \quad (26)$$

$$g = \frac{\nu_0}{(1 - e_{10}^2)} + \frac{\nu_1 x_0^2}{(1 - e_{10}^2)^2} + \nu_{21} \frac{\sqrt{1 - e_{10}^2}}{(1 - e_{20}^2)^{3/2}} - \nu_{22} \frac{(1 + 3e_{10}^2/2)}{(1 - e_{20}^2)^2}, \quad (27)$$

$$g_x = \nu_1 \frac{2x_0}{(1 - e_{10}^2)^2}, \quad (28)$$

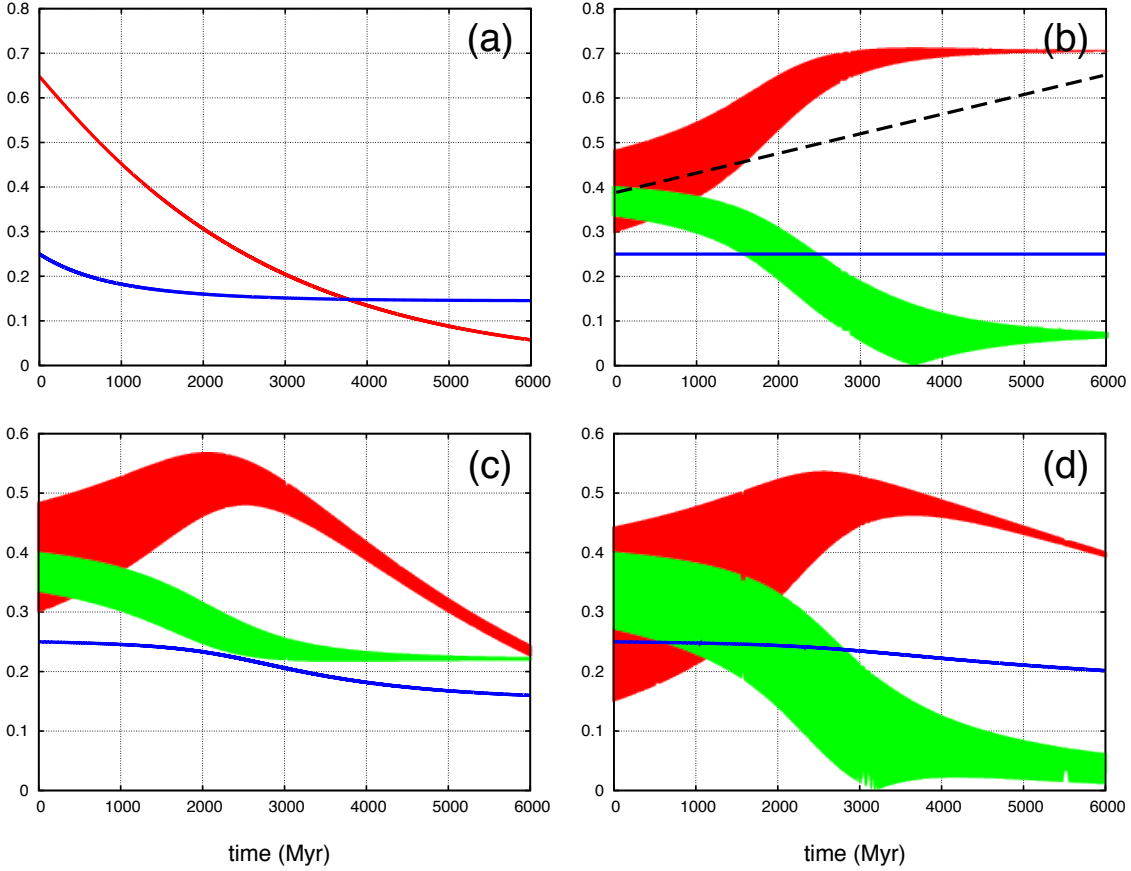


FIG. 1.— Long-term evolution of the HD 117618 system in different situations. We show the semi-major axis a_1 in AU (blue), and the eccentricities e_1 (red) and e_2 (green). (a) without a companion; (b) with a $m_2 = 0.2 M_J$ companion at $a_2 = 1.8$ AU, but without dissipation on the orbit; (c) same as (b), but with a full model; (d) with a $m_2 = 0.15 M_J$ companion at $a_2 = 1.4$ AU, with a full model. The dashed line gives the slope of the linear approximation (Eq. 37).

$$g_e = \nu_0 \frac{2e_{10}}{(1 - e_{10}^2)^2} + \nu_1 \frac{4x_0^2 e_{10}}{(1 - e_{10}^2)^3} - \nu_{22} \frac{3e_{10}}{(1 - e_{20}^2)^2} - \nu_{21} \frac{e_{10}}{\sqrt{1 - e_{10}^2}(1 - e_{20}^2)^{3/2}}, \quad (29)$$

$$\nu_x = K f_1(e_{10}), \quad (30)$$

$$\nu_e = -K(f_1'(e_{10})x_0 - f_2'(e_{10})), \quad (31)$$

where $f_1'(e) = 15(e + 3e^3/2 + e^5/8)/(1 - e^2)^{11/2}$, and $f_2'(e) = 3(9e + 65e^3/2 + 125e^5/8 + 5e^7/8)/(1 - e^2)^7$. We neglected the octupole terms since $\nu_{3i} \ll \nu_{2i}$, the contributions from δe_2 , and assumed that $e_{i0} \neq 0$.

At first order, the precession of the periastron is constant $\dot{\varpi} \simeq g$, and the eccentricity is simply given from expression (23) as

$$\delta e_1 = \Delta e \cos(gt + \varpi_0), \quad (32)$$

where $\Delta e = A/g$. That is, the eccentricity e_1 presents periodic variations around an equilibrium value e_{10} , with amplitude Δe and frequency g . Since $g_x \delta x, g_e \delta e_1 \ll g$, the above solution for the eccentricity can be adopted

as the zeroth order solution of the system of equations (23–25). With this approximation, the equation of motion of δx (25) becomes that of a driven harmonic oscillator whose the steady state solution is

$$\delta x = \Delta x \cos(gt + \varpi_0 - \phi), \quad (33)$$

with $\Delta x = \nu_e \Delta e / \sqrt{\nu_x^2 + g^2}$, and $\sin \phi = g / \sqrt{\nu_x^2 + g^2}$. The rotation rate thus presents an oscillation identical to the eccentricity (Eq. 32), but with smaller amplitude and delayed by an angle ϕ (see Correia 2011). Using the above expression in equation (24) and integrating, gives for the periastron:

$$\varpi = gt + \varpi_0 + \frac{g_x}{g} \Delta x \sin(gt + \varpi_0 - \phi) + \frac{g_e}{g} \Delta e \sin(gt + \varpi_0). \quad (34)$$

Finally, substituting in expression (23) and using the approximation $g_x \Delta x, g_e \Delta e \ll g$ gives

$$\delta \dot{e}_1 \approx -A \sin(gt + \varpi_0) - \frac{g_e A}{g} \Delta e \sin(gt + \varpi_0) \cos(gt + \varpi_0) - \frac{g_x A}{g} \Delta x \sin(gt + \varpi_0 - \phi) \cos(gt + \varpi_0), \quad (35)$$

or, combining the two products of periodic functions,

$$\begin{aligned} \delta \dot{e}_1 = & -A \sin(gt + \varpi_0) - \frac{g_x A}{2g} \Delta x \sin(2gt + 2\varpi_0 - \phi) \\ & - \frac{g_e A}{2g} \Delta e \sin(2gt + 2\varpi_0) + \frac{g_x A}{2g} \Delta x \sin \phi . \end{aligned} \quad (36)$$

The two middle terms in the above equation can be neglected since they are periodic and have a very small amplitude ($g_x \Delta x, g_e \Delta e \ll g$). However, the last term in $\sin \phi$ is constant and it adds a small drift to the eccentricity,

$$\langle e_1 \rangle = \frac{\nu_e g_x A^2}{2g(\nu_x^2 + g^2)} t . \quad (37)$$

The drift is maximized for $g \sim \nu_x$, it vanishes for weak dissipation ($\Delta x \rightarrow 0$), but also for strong dissipation ($\phi \rightarrow 0$). Note that the phase lag ϕ between the eccentricity (Eq. 32) and the rotation variations (Eq. 33) is essential to get a drift on the eccentricity. That is why the eccentricity pumping was never observed in previous studies that did not take into account the spin evolution.

The major difference when we consider the full non-linearized problem is that the drift (Eq. 37) cannot grow indefinitely. Indeed, when the eccentricity reaches high values, the drift vanishes (Fig. 1b). Moreover, tidal effects are also enhanced for high eccentricities and counterbalance the drift (Eq. 18). As a consequence, the drift on the eccentricity is never permanent, although it can last for the age of the system (Fig. 1c,d).

In order to observe the pumping effect, the eccentricity should not be damped, while the damping timescale of the spin of the planet should be of the order of the pe-

riod of eccentricity oscillation. This is valid for gaseous planets roughly within $0.1 < a_1 < 0.3$. About half of the planets in this range present eccentricities higher than 0.3 (Tab. 1). This is somehow unexpected, since the time-scale for damping the eccentricity ($\tau \sim 1/K'$) is shorter than the age of those systems (Tab. 1, Fig. 1a). Thus, unless the initial eccentricity of those planets was extremely high, one may suspect of the existence of undetected companions that help the eccentricity to maintain the present values.

5. CONCLUSION

In this Letter we have shown that, under some particular initial conditions, orbital and spin evolution cannot be dissociated. Indeed, counterintuitive behaviors can be observed, such as the secular augmentation of the eccentricity. This effect can last over long time-scales and may explain the high eccentricities observed for moderate close-in planets.

The variations in the flattening of the inner planet due to rotation (Eq. 1) is a key element to pump the eccentricity by means of g_x (Eq. 37). We have considered an instantaneous response to the rotation in J_2 , but a time delay until the maximum deformation is reached is to be expected. This may increase the phase lag between the eccentricity forcing (Eq. 32) and the precession angle oscillations (Eq. 34). It results that the drift effect on the eccentricity can be even more pronounced than the one presented here.

We acknowledge support from the PNP-CNRS, the FCT (grant PTDC/CTE-AST/098528/2008), and the European Research Council.

REFERENCES

- Butler, R. P., et al. 2006, *Astrophys. J.* , 646, 505
 Correia, A. C. M. 2009, *Astrophys. J.* , 704, L1
 Correia, A. C. M. 2011, in *IAU Symposium*, Vol. 276, IAU Symposium, ed. A. Sozzetti, M. G. Lattanzi, & A. P. Boss, 287
 Correia, A. C. M., & Laskar, J. 2004, *Nature* , 429, 848
 Correia, A. C. M., & Laskar, J. 2010a, *Icarus*, 205, 338
 Correia, A. C. M., & Laskar, J. 2010b, in *Exoplanets* (University of Arizona Press), 534
 Correia, A. C. M., Laskar, J., Farago, F., & Boué, G. 2011, *Celestial Mechanics and Dynamical Astronomy*, 111, 105
 Correia, A. C. M., Laskar, J., & Néron de Surgy, O. 2003, *Icarus*, 163, 1
 Efroimsky, M., & Williams, J. G. 2009, *Celestial Mechanics and Dynamical Astronomy*, 104, 257
 Lambeck, K. 1988, *Geophysical geodesy : the slow deformations of the earth* Lambeck. (Oxford [England] : Clarendon Press ; New York : Oxford University Press, 1988.)
 Laskar, J., & Boué, G. 2010, *Astron. Astrophys.* , 522, A60
 Laskar, J., Boué, G., & Correia, A. C. M. 2011, arXiv:1110.4565
 Lee, M. H., & Peale, S. J. 2003, *Astrophys. J.* , 592, 1201
 Mardling, R. A. 2007, *Mon. Not. R. Astron. Soc.* , 382, 1768
 Mignard, F. 1979, *Moon and Planets*, 20, 301
 Murray, C. D., & Dermott, S. F. 1999, *Solar System Dynamics* (Cambridge University Press)
 Singer, S. F. 1968, *Geophys. J. R. Astron. Soc.* , 15, 205
 Touma, J. R., Tremaine, S., & Kazandjian, M. V. 2009, *Mon. Not. R. Astron. Soc.* , 394, 1085